

ATOMIC MODELLING OF CHEMICAL INTERACTIONS AT CRACK TIPS

E. R. FULLER Jr, B. R. LAWN† and R. M. THOMSON

Fracture and Deformation Division, National Bureau of Standards, Washington, D.C. 20234, U.S.A.

(Received 11 February 1980)

Abstract—A simple atomic model for incorporating the effects of chemically-assisted fracture is described. Development of the model is in two parts, which can be formulated independently: (i) the crack itself is represented by two elastic semi-infinite chains of atoms, linked transversely by stretchable bonds (quasi-one-dimensional representation); (ii) the chemical interaction, which takes place at the crack tip atoms, is represented by a classical reaction between two diatomic molecules. While clearly oversimplistic in relation to real structural materials, the approach offers insight into the actual mechanisms of crack-tip chemistry. In particular, the factors which contribute to the generalised force on the crack-tip bond (viz. the applied load, the lattice, and the cohesive force itself) are clearly identified, and conclusions may be drawn in a quite general way about the prospective response of alternative crack systems. The mechanisms of chemically-assisted crack growth under either equilibrium or kinetic conditions are contained naturally in the formalism. Although explicitly set up along the lines of an ideally brittle crystalline cleavage, the model may well be extended to traditionally more complex crack configurations, e.g. as in glasses and metals.

Résumé—Nous présentons un modèle atomique simple pour tenir compte des effets de la rupture assistée chimiquement. Le modèle est articulé en deux parties, qui peuvent être présentées indépendamment: (i) la fissure proprement dite est représentée par deux chaînes d'atomes élastiques semi-infinies, reliées transversalement par des liaisons extensibles (représentation quasi-unidimensionnelle); (ii) l'interaction chimique sur les atomes de l'extrémité de la fissure est représentée par une réaction classique entre deux molécules diatomiques. Bien qu'elle soit évidemment simpliste par rapport à la structure des matériaux réels, cette approche permet d'étudier les mécanismes réels de la chimie à l'extrémité de la fissure. En particulier, les facteurs qui contribuent à la force généralisée sur la liaison à l'extrémité de la fissure (à savoir la charge appliquée, le réseau et la force de cohésion elle-même) sont clairement identifiés et l'on peut tirer des conclusions assez générales sur la réponse attendue d'autres systèmes à fissure. Les mécanismes de la croissance des fissures assistée chimiquement dans des conditions cinétiques ou d'équilibre sont naturellement contenus dans ce formalisme. Bien qu'il soit explicitement établi le long des lignes d'un clivage cristallin idéalement fragile, ce modèle peut être étendu à des configurations de fissures plus complexes, comme c'est le cas dans les verres et dans les métaux par exemple.

Zusammenfassung—Ein einfaches atomistisches Modell wird beschrieben, welches die Effekte chemisch unterstützten Bruches umfaßt. Das Modell wird in zwei unabhängig formulierbaren Stufen entwickelt: (i) der Riß selbst wird dargestellt mit zwei elastischen halbunendlichen Atomketten, die miteinander über dehnbare Bindungen zusammenhängen (quasi-eindimensionale Darstellung), (ii) die an den Atomen der Rißspitze angreifende chemische Wechselwirkung wird als klassische Reaktion zwischen zwei diatomaren Molekülen dargestellt. Wenn auch zu stark vereinfacht in Hinsicht auf reale Materialien, so liefert diese Näherung doch Einsichten in die an der Rißspitze tatsächlich ablaufenden chemischen Mechanismen. Insbesondere werden die Faktoren, die zur generalisierten Kraft auf die Bindungen an der Rißspitze beitragen (d.h. die angelegte Last, das Gitter und die Kohäsion selbst) aufgefunden; auf das voraussichtliche Verhalten alternativer Rißsysteme kann in ganz allgemeiner Weise geschlossen werden. Die Mechanismen chemisch unterstützter Rißausweitung sowohl unter Gleichgewichts- als auch kinetischen Bedingungen werden von diesem Formalismus miteerfaßt. Das Modell, das explizit für Bedingungen ideal spröder Kristallspaltung formuliert ist, kann auf komplexere Rißkonfigurationen z.B. in Gläsern und Metallen ausgeweitet werden.

1. INTRODUCTION

The quest for an understanding of fracture processes at a fundamental level has provided considerable impetus to the atomic modelling of crack tips (for reviews, see Refs. [1–5]). Even simplistic models, [6] while perhaps not directly applicable to 'real' structures, usefully demonstrate the connection between

macroscopic fracture parameters (e.g., elastic modulus, surface energy) and interatomic force laws, and thereby serve as a basis for predicting crack response from first principles. Moreover, the solutions of the equilibrium equations for the discrete-structure models show one major feature not apparent in their continuum counterparts—the existence of atomic energy barriers to crack growth ('lattice trapping'), a concept central to any discussion of thermally-activated fracture. Although most attention to date has been directed to

† On study leave from University of New South Wales Australia.

the intrinsic barriers which occur naturally in isolated crack-tip systems, by far the most important practical manifestation of activated crack growth is that which owes its origin to the weakening effect of an extraneous chemical species. The present study accordingly seeks to extend the base of the atomistic models to allow the incorporation of crack-tip chemistry.

Our approach here, foreshadowed in recent treatments of lattice trapping models [7, 8], is to work with a system which minimizes mathematical complication, yet does not exclude general conclusions. The basic idea is essentially a combination of two separate developments: (i) with proper choice of coordinate system, the solutions for the displacements of linearly-connected atoms in an equilibrium crack system can be effectively decoupled from the nonlinear force function which determines the rupture of crack-tip bonds, thus providing for complete flexibility in the choice of interaction process for crack-tip atom pairs [5]; (ii) the interaction between any such crack-tip atom pair and an extraneous molecular species may be conveniently described in terms of displacements in configurational-energy space [2, 8], in the classical manner of chemical reaction-rate theory [9]. Our specific model, therefore, is similar to the quasi-one-dimensional chain representation of earlier work [6] but with the crucial crack-tip atom pair treated as an embedded diatomic molecule free to interact with a second molecule from the environment. This approach conveniently allows for recourse to well-established formalisms of the lattice-mechanical and chemical aspects of the problem.

One of the major underlying aims of the current study is to present a framework for rationalizing the ostensibly complex nonlinear processes which contribute to the broad phenomenon of brittle fracture. The central point of our argument is the 'sharp-crack' concept, i.e. brittle cracks grow via the sequential rupture of cohesive bonds at the crack tip. There is now compelling evidence, both theoretical [3] and experimental [10], to indicate that this is certainly the mechanism of fracture in strongly-bonded, covalent/ionic structures (ceramics) at room temperatures; indeed, there is a growing school of thought which suggests that the sharp-crack concept may retain its validity in metallic structures, even in cases where ('non-blunting') flow processes about the tip account for the greater part of the material toughness [11-14]. In this context, the model allows us to draw some conclusions concerning the influence of atomic structure (including that of the environmental species) on crack growth characteristics. Again, the one-dimensional form of the analytical solutions given explicit consideration here is not necessarily restrictive: the 'embedded diatomic molecule' notion would appear to be equally valid in describing the interaction at, say, a kink site on an extended crack front—only the elastic response of the constraining structure would differ. Similarly, we focus our attention on equilibrium configurations, in the knowledge

that, once the activation energies for bond rupture are evaluated, kinetic effects may be determined by the conventional methods of statistical thermodynamics [8].

2. EQUILIBRIUM SOLUTIONS OF ONE-DIMENSIONAL MODEL

In this section the mechanical stability of the quasi-one-dimensional crack model is investigated, first in the absence of any chemical environment and then with potentially reactive species present at the critically strained bonds.

2.1 Intrinsic bond rupture

Consider the atomistic model shown in Fig. 1, after Thomson *et al.* [6]. The atoms are bonded in two semi-infinite chains by bendable (longitudinal) and stretchable (transverse) spring elements. Opening forces P at the free ends of the chains produce displacements u_0 at the crack mouth, thereby doing mechanical work on the system. The stretchable elements up to the n th bond are assumed to be 'broken', i.e. stretched beyond their range of interaction, thus defining a finite crack length. We shall assume all spring elements to be linear in their force/displacement response, except for the crack-tip bond itself which is necessarily nonlinear. Of course, once the n th bond has parted, the next bond becomes the most highly strained element in the system, and accordingly takes up the nonlinear configuration of its predecessor.

To determine the equilibrium conditions for this system [5-7] we must first specify the characteristics of the spring elements, Fig. 2. For any stretchable bond j the required information is contained in the interatomic force function $f_b(u_j)$ or potential energy

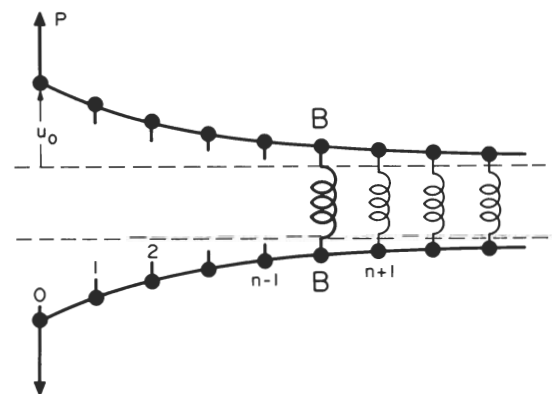


Fig. 1. Quasi-one-dimensional model of a crack. Atoms are linked longitudinally by bendable elements, and transversely by stretchable elements; only the transverse element BB, representing the crack-tip bond, is considered to be displaced in a region of nonlinear response.

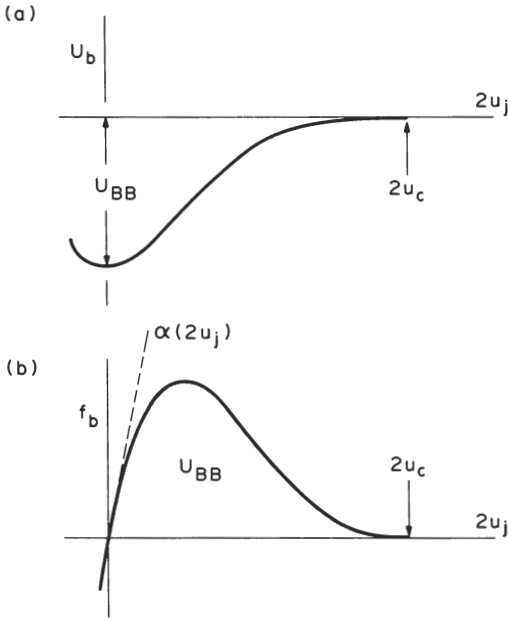


Fig. 2. Potential energy and force functions for bonds stretched across crack plane. Note in the $f_b(u_j)$ plot that the initial slope gives the stiffness, and the area under the curve the bond-rupture energy.

function $U_b(u_j)$, where†

$$f_b = \partial U_b / \partial (2u_j). \quad (1)$$

Then for displacements within the linear region we may define an elastic stiffness constant

$$\alpha = [df_b/d(2u_j)]_{u_j=0} \quad (2)$$

Again, we may define a bond-rupture energy for displacements to the cutoff limit

$$U_b^* = \int_0^{2u_c} f_b d(2u_j) = U_{BB}; \quad (3)$$

i.e. the energy required to rupture the bond reversibly is simply the intrinsic cohesive energy. For the bendable elements we specify a spring (rigidity) constant β representing resistance to angular distortion of the bonds which link at j . The total potential energy of the crack system thus takes the form

$$U = -2Pu_0 + \beta \sum_{j=1}^{\infty} (u_{j+1} - 2u_j + u_{j-1})^2 + nU_{BB} + \int_0^{2u_n} f_b d(2u_n) + 2\alpha \sum_{j=n+1}^{\infty} u_j^2. \quad (4)$$

The first term on the right-hand side is the potential energy of the loading system; the second term is the

strain energy in the bendable elements; the remainder of the terms pertain to the stretchable elements, representing respectively contributions from bonds behind, at, and ahead of the tip. At given applied load and crack length the conditions for equilibrium are

$$\partial U / \partial (2u_j) = 0 \quad (j = 0, 1, \dots, \infty), \quad (5)$$

which corresponds to an infinite set of fourth-order difference equations. Analytical solutions of the functional form $u_j(P, n, u_n)$ are obtainable for all but the crack-tip bond, i.e. for all $j \neq n$.

Combination of these equilibrium-displacement solutions accordingly reduces the system potential energy to an explicit function of the crack-tip displacement u_n which may be varied arbitrarily:

$$U_n = -2P(1 + n/\xi)u_n - (P^2/6\beta)n(2n^2 + 3n\xi + 1) + nU_{BB} + U_b(u_n) + (\xi - 1)\alpha u_n^2 \quad (6)$$

where $\xi = \{[1 + (1 + 8\beta/\alpha)^{1/2}]/2\}^{1/2}$ is a composite elastic coefficient. We may now define a generalised net force for crack-tip bond rupture,

$$F_n = -\partial U_n / \partial (2u_n) = P(1 + n/\xi) - f_b(u_n) - (\xi - 1)\alpha u_n; \quad (7)$$

for $F_n > 0$ the bond opens, for $F_n < 0$ it closes.

This result is particularly useful for demonstrating the interrelationships between the factors which contribute to intrinsic bond rupture in brittle fracture. The first, positive term on the right-hand side of equation (7) represents the applied driving force for the fracture; the second and third, negative terms represent the resisting forces. The third term is of special interest here: it corresponds to the restoring force exerted on the crack-tip atoms by the remainder of the (linear) structure, and simply augments the restoring force supplied by the nonlinear connecting bond. We may note that this 'lattice' force is uniquely determined by the elastic spring constants of the constituent elements – it contains no explicit information on the atomic displacements other than those at the crack tip itself. Consequently, the structure may be considered in terms of an equivalent linear elastic 'continuum', of stiffness $(\xi - 1)\alpha$, into which the separating crack-tip atoms BB are embedded.

It is instructive to consider the graphical representations of the system force functions in Fig. 3. The solid curves in Fig. 3a are composite plots of the restoring force terms, i.e. the nonlinear cohesive term $f_b(u_n)$ and the linear constraint term $(\xi - 1)\alpha u_n$ [5]. The three cases depicted correspond to different β/α ratios (the lowest curve representing the zero-rigidity limit, $\beta = 0$, and the highest curve conversely representing a high-rigidity extreme†, $\beta \gg \alpha$). We focus our attention on the intermediate case, which is seen to possess a maximum and a minimum. Figure 3b is a plot of the

† We adopt the definition in equation (1) with a conventional negative sign omitted as a matter of convenience, in order that $f_b > 0$ for all $u_j > 0$; it is thereby to be understood that positive f_b represents a *restoring* cohesive force.

‡ E. Smith [15] has recently purported to show that lattice trapping must exist in any discrete structure, in which case the upper curve in Fig. 3(a) may not represent a realistic configuration.

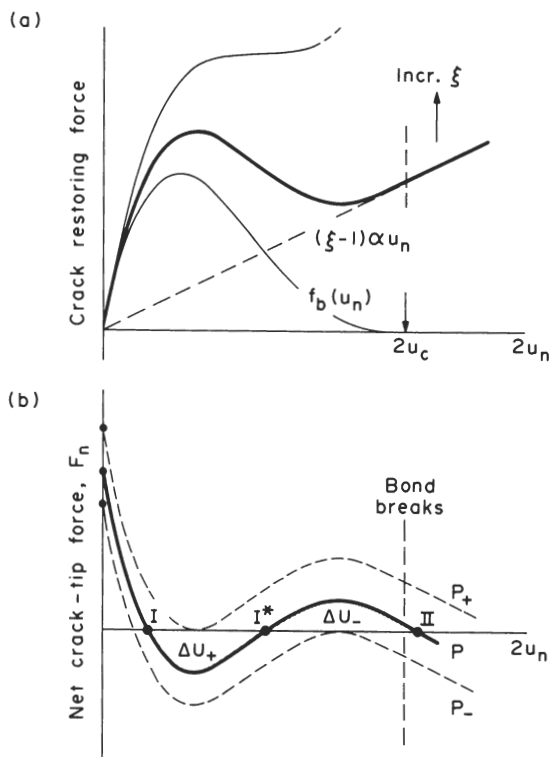


Fig. 3. Graphical construction showing (a) restoring force, and (b) net bond-rupture force, as function of crack-tip displacement. Curves are representations of equation (7) for intrinsic bond rupture.

net-force function equation (7) for this particular case: the construction here is made simply by inverting the restoring-force curve, and relocating its origin a distance $P(1 + n/\xi)$ along the ordinate. According to this description, the effect of increasing the applied load P may be conveniently represented by displacing the entire curve vertically upward on the plot. The requirement that the crack-tip displacement correspond to an equilibrium configuration, i.e. $F_n = 0$, is satisfied where the curve intersects the abscissa. Thus, in general, there exists a range of applied loads $P_- < P < P_+$ for which there are three equilibrium configurations. The equilibria corresponding to configurations I and II are seen to be stable: at I, the atoms at $j = n$ are held together predominantly by the cohesive forces – i.e. the bond is ‘intact’; at II, it is the constraint of the surrounding structure which dominates – i.e. the bond is ‘broken’, and the crack has advanced through one complete atomic spacing. Likewise, the intervening equilibrium configuration I^* is unstable. In terms of this picture, we may identify the load P_+ (where solutions I and I^* coalesce) with the critical condition for spontaneous crack *advance*, and P_- (where II and I^* coalesce) similarly with the critical condition for crack *retreat*.

The model also provides the necessary quantities for a description of thermal effects in brittle fracture. In line with equation (7), the shaded areas under the curve in Fig. 3b correspond to forward (bond break-

ing) and backward (bond remaking) energy barriers for the system at given load P and crack size n :

$$\Delta U_+ = U_n^* - U_n^I = - \int_I^{I^*} F_n d(2u_n) \quad (8a)$$

$$\Delta U_- = U_n^* - U_n^{II} = - \int_{II}^{I^*} F_n d(2u_n). \quad (8b)$$

True thermal equilibrium then obtains at $\Delta U_+ = \Delta U_-$, which defines the quiescent crack configuration appropriate to the Griffith energy-balance notion. The individual contributions of the terms in the force function equation (7) (i.e. the applied loading, cohesive, and lattice terms) to the barrier heights may be deduced graphically from Fig. 3. A more formal evaluation of the integrals in equation (8) requires an analytical expression for the nonlinear function $f_b(u_n)$ – specific examples are treated elsewhere [5, 6, 8].

The construction of Fig. 3 lends itself to ready adaptation to the concepts of crack-tip chemistry. Thus, passage from the stable crack configuration I to the equivalent configuration II may be deemed to proceed along the ‘reaction coordinate’ $2u_n$ via the ‘activated complex’ configuration I^* . In a more generalised configurational-space representation, the system potential energy function $U(u_0, u_1, \dots)$ possesses a series of local minima corresponding to successive positions of the advancing tip; the reaction path then becomes a complex function of successive crack-tip displacements, progression from one energy minimum to the next occurring via a saddle point in the hyperspace [8].

2.2 Extrinsic (chemically-assisted) bond rupture

Now let us adapt the model to allow for chemical interactions at the crack-tip bond. To this end, we make special note of the simple manner in which the nonlinear force term f_b enters equation (7): chemistry may thus be accommodated exclusively via this term, without in any way affecting the applied loading and lattice contributions to the total force function. In other words, the *mechanics* of fracture are the same as before – only the *mechanism* is different, so the problem reduces to one of determining a suitable cohesive force representation for any specified interaction process.

For simplicity, the system we take as our basis for discussion is that illustrated in Fig. 4. [2] An environmental molecule A–A interacts with the crack-tip bond –B–B–, producing ‘terminal’ bonds A–B–. Since we are free to consider any such crack-tip event independently of the remainder of the crack system, we may conveniently regard the rupture process in terms of the well-studied reaction between diatomic gas molecules, $AA + BB \rightarrow 2AB$ [16]. All bonds broken in this way are saturated at the free crack surfaces, so incoming molecules remain relatively inactive until they arrive at freshly exposed atoms at the tip. Implicit in our description is, of course, the

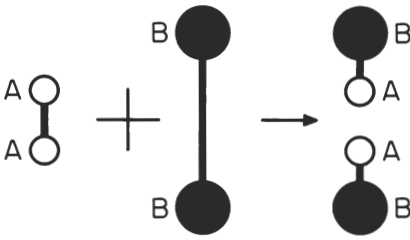


Fig. 4. Schematic of chemically-induced bond rupture. Extraneous molecule AA reacts with crack-tip bond BB to produce 'terminal' bonds AB.

assumption that one molecule interacts with one bond in a single-step process—however, while departures from this assumption must inevitably introduce added complexities into the analysis, the basic approach is expected to be quite general.

The interatomic potential energy and force characteristics for the 'diatomic-molecule' representation are depicted in Fig. 5. In this diagram the curves are plotted as a function of B–B separation, with AA adjusted to a position of minimum energy at each point along the 'reaction coordinate' $2u_j$. Thus for small crack-tip displacements u_j , the atoms BB are only slightly perturbed from their initial bond configuration, the molecule AA assuming an equilibrium position some atom spacings distant in accordance with a weak van der Waals interaction. The energy curve depicting the unreacted state AA + BB will therefore differ little in shape from that for an isolated bond B–B, Fig. 2. On the other hand, for large u_j , such that B–B is effectively dissociated, conditions are more favourable to the formation of A–B bonds. The energy curve depicting the reacted state 2AB will then tend to rise as the BB separation diminishes, owing to polar repulsion of the like AB configurations across the separation plane. At any given B–B separation the appropriate energy state will be determined by the lower of the two curves in Fig. 5a, with rounding off at the cross-over point due to resonance between the two configurations. From the equivalent representation of this crossover phenomenon in the force/separation plot of Fig. 5b, we see that the elastic stiffness of the BB bond is essentially the same as before, equation (2). However, the bond-rupture energy required to take the crack-tip atoms reversibly from their initial bound state to the final reacted state is significantly modified for all $2U_{AB} > U_{AA}$ †

$$U_b^* = \int_0^{2u_c'} f_b d(2u_j) = U_{AA} + U_{BB} - 2U_{AB} \quad (9)$$

where $2u_c'$ is the cutoff displacement for the 2AB force curve. The value of U_b^* may thus be much less than the quantity U_{BB} appropriate to intrinsic bond rupture, equation (3), and may even become negative.

† If $2U_{AB} < U_{AA}$ the potential energy curves in Fig. 5a never cross, in which case U_b^* is given as before by Equation (3).

Now let us fold in the modified cohesive force term with the applied loading and lattice constraint terms to obtain the net crack-tip force function F_n in equation (7). The procedure is the same as that used in constructing Fig. 3. Fig. 6a shows composite plots of the restoring force terms due to the bond and the constraining lattice, and Fig. 6b the corresponding net crack-tip force function. (The curves relating to intrinsic bond rupture, included for the sake of comparison, are plotted for the same lattice conditions as previously.) The stable equilibria corresponding to configurations I and II now relate explicitly to the unreacted and reacted (adsorption) states of the bond respectively; the unstable configuration I* accordingly relates to the activated complex state of the crack-tip reaction $AA + BB \rightarrow 2AB$. Recalling that the origin of the $F_n(u_n)$ curve is displaced an amount $P(1 + n/\$)$ along the ordinate, and that there is a range of loads $P_- < P < P_+$ (not indicated in Fig. 6b) within which the crack is effectively trapped by the structure, it is apparent that the general effect of the chemical interaction is to reduce the applied forces necessary to drive the crack. Insofar as propagation under conditions of mechanical equilibrium is concerned, both the critical loads for advance, P_+ ,

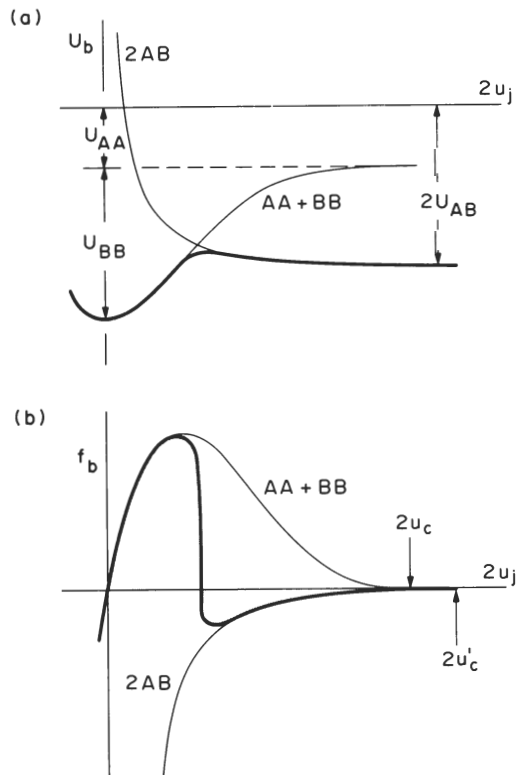


Fig. 5. Potential energy and force functions for bonds subjected to reaction in Fig. 4. Heavy curves represent minimum energy state for any given BB bond displacement—note crossover from AA + BB curve to 2AB curve at critical displacement (activated complex). Note also the reduction in bond-rupture energy (area under $f_b(u_j)$ curve) resulting from the interaction.

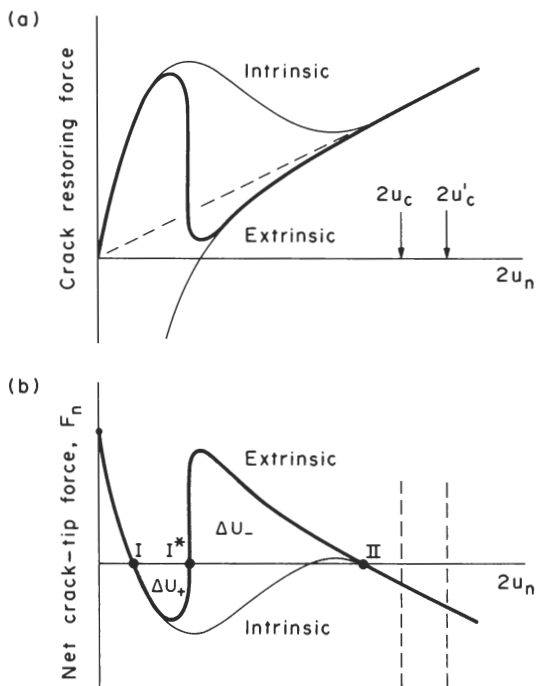


Fig. 6. Graphical construction showing (a) restoring force, and (b) net bond-rupture force as function of crack-tip displacement. Curves are representations of equation (7) for extrinsic bond rupture. Effect of chemical interaction is to enhance the forces driving the bond-rupture process.

and retreat (i.e. spontaneous desorption of the AA molecule), P_- , are lowered (P_+ only slightly, for the particular case illustrated). With regard to thermally activated propagation, the pertinent result is that the energy barrier [see equation (8)] to forward motion, ΔU_+ , is lowered, and to backward motion, ΔU_- , is raised: the load at the quiescent point, i.e. corresponding to the thermal equilibrium condition $\Delta U_+ = \Delta U_-$, is therefore also lowered.

It is of some interest to examine the effect of the "strength" of the chemical interaction, as measured by

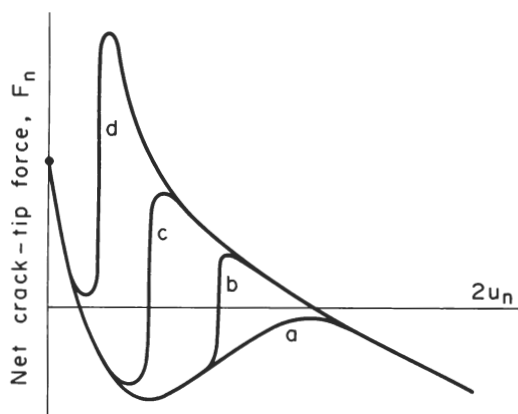


Fig. 7. Net bond-rupture force for crack-tip displacement, showing effect of "strength" of chemical interaction on lattice trapping limits. Curves *a, b, c, d* represent increasing values of $2U_{AB} - U_{AA}$.

the quantity $2U_{AB} - U_{AA}$ in Fig. 5a [i.e. the difference between the intrinsic and extrinsic bond-rupture energies in equations (3) and (9)], on the crack-tip force characteristics. The plots in Fig. 7 are for different values of this quantity, starting at zero for curve *a* (intrinsic) and increasing through the sequence *b, c, d*. For the particular load P and crack size n represented in the figure, the crack in system *a* would be subject to spontaneous retreat, in *b* to activated advance, in *c* to activated advance, and in *d* to spontaneous advance. If the interaction is weak, as in system *b*, the critical load P_+ required to extend the crack at mechanical equilibrium may differ imperceptibly from that which obtains in intrinsic bond rupture (note near-coincident minima in curves *a* and *b*), even though the corresponding load P_- for retreat is substantially reduced. If the interaction is strong, as in system *d*, not only does P_+ now diminish, but P_- tends to become negative (cf. maximum in curve with intercept on ordinate); in this extreme the interaction is irreversible (desorption of the molecule AA apparently requiring the bond force to be applied compressively). Overall, chemistry acts to displace the activated complex configuration toward smaller atom separations at the crack tip, with consequent reduction in the load at which true Griffith equilibrium maintains.

3. DISCUSSION

We have developed a quasi-one-dimensional model, based on a linear atomic chain construction, for examining the effect of material discreteness on brittle fracture. In particular, noting that for a given loaded system the crack-tip displacement uniquely determines the crack driving force [equation (7)], we have been able to introduce chemistry into the problem by regarding the separating crack-tip bond as an active diatomic molecule. Although clearly oversimplistic in relation to real brittle fracture systems, our specific model does show several characteristics which would appear to be quite general. The implications arising from some of these characteristics are worth examining from the standpoint of the fracture-mechanics/fracture-mechanism dichotomy.

First, we may note that our analysis has been carried out entirely in terms of atomic structural parameters. In the limit of $n \rightarrow \infty$, $b_0 \rightarrow 0$, where b_0 is the interatomic spacing, the solutions should reduce to their more conventional continuum counterparts. This limit is readily evaluated, in the approximation of linear elasticity, if it is required that the crack length $c = nb_0$ and the elastic constants of the structure retain sensible (non-zero, non-infinite) values [7]: the equilibrium condition, corresponding to $F_n = 0$ and $(\partial U_n / \partial c) = 0$, becomes $P(c + b_0 \delta) = b_0 (\beta U_b)^{1/2}$. Defining a 'surface energy density' (per unit length of crack), $2\gamma = U_b / b_0$, this expression reduces to the standard continuum relation for crack equilibrium, $G = 2\gamma$, if we also define a corresponding 'crack

extension force' $G = P^2(c + b_0\delta)^2/\beta b_0^3$ (with βb_0^3 constant, averaged over all elements in the structure): this last relation is indeed identical in form to that obtained for the well-known, double-cantilever test beam configuration [17].

The question that may now be asked is, what does the linear parameter G measure in a test on a discrete structure such as in Figs. 1 and 4? Returning to equation (7), we may note that the term $P(1 + n/\xi)$ in the crack-tip force function is independent of u_n – it contains no information at all about events at the crack tip. Thus in the constructions of Figs. 3b and 6b the intercept of the force curve on the ordinate is effectively determined by the structure-insensitive quantity G . The *shape* of the force curve is determined primarily, of course, by the functions which define the crack-tip response, i.e. $f_b(u_n)$ or $U_b(u_n)$. The underlying basis of the lattice trapping phenomenon is therefore expected to reflect in the surface energy term γ . Accordingly, measurements of critical loads for crack extension under different equilibrium conditions can provide varied information on the effective value of this surface energy. At *mechanical* equilibrium, the critical load measures the upper trapping limit, giving $G_+ = 2\gamma_+$; at *thermal* equilibrium, it is the configuration at which forward and backward fluctuations are equally probable which pertains, so that $G_0 = 2\gamma_0$, where $2\gamma_0 = U_b^*/b_0$ is the truly reversible surface energy in the classical Griffith sense. In this description, $\gamma_- \leq \gamma_0 \leq \gamma_+$ always (see Fig. 3b). (In more practical fracture mechanics parlance, γ_+ is a measure of 'toughness', K_{IC} ; γ_0 is a measure of the fatigue limit in so-called 'stress corrosion cracking', K_{ISCC} .) More detailed discussions of the relations between fracture criteria at the macroscopic and microscopic levels, including the functional form of the crack velocity $v(K)$ within the trapping range, are given elsewhere [5, 8].

Next, let us consider the implications of the analysis concerning the role of structure on the fracture response. We have already alluded, via Fig. 3, to a possible elimination of intrinsic lattice trapping for structures with sufficiently large values of β/α . [5, 6, 15]. (Incidentally, a careful examination of Figs. 3 and 6 indicates that a crack system which shows no *intrinsic* lattice trapping may still show strong *extrinsic* trapping.) Again, in our discussion of equation (7) in section 2.1 it was pointed out that the constraint of the 'lattice' on the separating crack-tip bond may be considered in terms of an equivalent continuous matrix of stiffness $(\xi - 1)\alpha$. This stiffness represents an averaged value over all elements in the system, so essentially the same result would obtain if the linear matrix were to be replaced by a two- or three-dimensional continuum of identical elastic response. In other words, there is nothing in the analysis to suggest that plots of the type shown in Figs. 3 and 6 might not be equally applicable to an active bond at, say, a kinked crack front in a crystal cleavage configuration. General lattice trapping charac-

teristics have in fact been observed in two- and three-dimensional crack models [18, 19]. Further, it may be argued in the same vein that the assumptions of perfect linearity and atomic periodicity in the lattice (implicit in the derivation of equation (7)) are unlikely to be highly restrictive. Nonlinearity in the lattice elements should be significant only in the immediate vicinity of the crack-tip bond, and is therefore not expected to reflect strongly in the averaged stiffness which determines the overall lattice response; nonperiodicity, likewise, may be suitably averaged in the lattice term by using macroscopically-determined elastic constants. Such factors, of course, must be given explicit consideration in the specification of the function $f_b(u_n)$ for the crack-tip bond: we have indicated earlier (section 2.1) that nonlinearity in this function is a necessary input into any physically realistic theory of brittle fracture; structural nonperiodicity, e.g. glasses, may be simply accommodated, in principle, by means of an appropriate distribution of such functions over the crack plane.

Similar conclusions may be drawn concerning the detailed nature of chemically-induced bond rupture at the crack tip. Our analysis based on the classical reaction between two diatomic molecules ignores several possible complications. First, the chemical bond at the crack tip will surely be influenced by the surrounding structure. Then, once reaction has occurred, the bond structure on the new free surface may be subject to substantial rearrangement. Again, the reaction may not proceed in a single step, but rather in a series of substeps along a complex reaction path. Nevertheless, none of these complications detracts from the scheme of Fig. 6 as a means for describing the basic mechanisms of bond weakening: it is only the exact form of the cohesive function $f(u_n)$ which varies. For instance, if the molecule AA in Fig. 4 were to dissociate *prior to* reacting with bond BB, e.g. by virtue of a precursor state of physisorption on the adjacent crack walls, we might anticipate the curves in Fig. 5a to remain a reasonable representation of the rupture event, but with that labelled 2AB displaced upward in accordance with $U_{AA} \rightarrow 0$. In the construction of Fig. 7 the effect of systematically reducing U_{AA} relative to $2U_{AB}$ is simply to displace the curves through the sequence $b \rightarrow c \rightarrow d$. The greatly enhanced crack growth observed in steels when gaseous hydrogen is introduced into the environment in atomic rather than molecular form [20] may be a manifestation of this type of weakening phenomenon.

Finally, it needs to be re-emphasised that the usefulness of the atomic models described in this study rests with the validity of the underlying sharp-crack concept. We mentioned in the Introduction the existence of evidence supporting this concept in materials which fail by a highly brittle mode, notably ceramics. It was also mentioned that the concept might logically be extended to metallic structures, notwithstanding the acknowledged fact that extensive flow pro-

cesses are capable of absorbing most of the work to fracture. Central to this line of thinking is the condition that the flow process cause no blunting of the crack tip *at the atomic level* – indeed, it can be argued that the requirements for such blunting are stringent, and are likely to be met as the exception rather than the rule [21]. The processes of plasticity then enter the description via the mechanics, not the mechanisms, of fracture. Thus, specific models proposed by Thomson, Hart and Weertman envisage a ‘shielding’ role for the plastic zone, in which the actual stress field experienced at the tip is substantially reduced below that one might estimate from applied-load and crack-geometry considerations [11–14]. This leaves the fundamental processes which actually control crack growth to be explained in terms of atomistic models. It is in this context that the simplistic ideas expressed in Figs. 1 and 4 might ultimately be expected to have a wider application, e.g. in the complex area of metal embrittlement by hydrogen or liquid metal environments.

Acknowledgements—The authors wish to acknowledge stimulating discussions with Ed Hart on the role of plasticity in brittle fracture—the final paragraph above inevitably reflects his ideas on the topic.

REFERENCES

1. R. M. Thomson, *Ann. Rev. Mater. Sci.* **3**, 31 (1973).
2. B. R. Lawn and T. R. Wilshaw, *Fracture of Brittle Solids*, Ch. 7. Cambridge University Press, London (1975).
3. R. M. Thomson, *The Mechanics of Fracture* Vol. 19, p. 1. (Edited by F. Erdogan), New York (1977).
4. E. Smith, *Fracture* Vol. 4, p. 65. (Edited by D. M. R. Taplin) University of Waterloo Press, Canada (1977).
5. E. R. Fuller and R. M. Thomson, *Fracture Mechanics of Ceramics*, Vol. 4, p. 507. (Edited by R. C. Bradt, D. P. H. Hasselman and F. F. Lange) Plenum, New York (1978).
6. R. M. Thomson, C. Hsieh and V. Rana, *J. appl. Phys.* **42**, 3154 (1971).
7. E. R. Fuller and R. M. Thomson, *Fracture* Vol. 3, p. 387. (Edited by D. M. R. Taplin) University of Waterloo Press, Canada (1977).
8. R. M. Thomson and E. R. Fuller, *J. Mater. Sci.* **15**, 1014 and 1027 (1980).
9. S. Glasstone, K. J. Laidler and H. Eyring, *The Theory of Rate Processes*. McGraw-Hill, New York (1941).
10. B. R. Lawn, B. J. Hockey and S. M. Wiederhorn, *J. Mater. Sci.* **15**, 1207 (1980).
11. R. M. Thomson, *J. Mater. Sci.* **13**, 128 (1978).
12. E. Hart, *Int. J. Solids Struct.*, in press.
13. J. Weertman, *Acta Met.* **26**, 1731 (1978).
14. J. Weertman, *J. Mater. Sci.*, in press.
15. E. Smith, *Int. J. Fract. Mechan.* **15**, R87 (1979).
16. J. C. Slater, *Introduction to Chemical Physics*, Ch. 10. McGraw-Hill, New York (1939).
17. B. R. Lawn and T. R. Wilshaw, *Fracture of Brittle Solids*, Ch. 3. Cambridge University Press, London (1975).
18. C. Hsieh and R. M. Thomson, *J. appl. Phys.* **44**, 2051 (1973).
19. D. M. Esterling, *J. appl. Phys.* **47**, 486 (1976).
20. H. G. Nelson, D. P. Williams and A. S. Tetelman, *Metall. Trans.* **2**, 953 (1971).
21. J. R. Rice and R. M. Thomson, *Phil. Mag.* **29**, 73 (1974).